Dynamic-mode scanning force microscopy study of n-InAs(110)-(1×1) at low temperatures

A. Schwarz, W. Allers, U. D. Schwarz, and R. Wiesendanger
Institute of Applied Physics and Microstructure Research Center, University of Hamburg, Jungiusstrasse 11, D-20355 Hamburg, Germany
(Received 15 July 1999)

We present results of an atomic-scale study on *in situ* cleaved InAs(110) in the dynamic mode of scanning force microscopy (SFM) at low temperatures. On a defect-free surface, the dynamic mode SFM images always exhibit strong maxima above the positions of the As atoms, where the total valence charge density has its maximum. Occasionally, with certain tips, the In atoms also become visible. However, their appearance strongly depends on the specific tip-sample interaction: We observed protrusions as well as depressions at the position of the In atoms. In this context, the role of the charge rearrangements induced by the specific electronic structure of the tip on the contrast in atomic-scale images is discussed in detail. Additionally, we investigated the appearance and nature of two different types of atomically resolved point defects. The most frequently observed point defect manifests itself as a missing protrusion, indicating the existence of an As vacancy. A second type of point defect is probably an In vacancy, which could be detected indirectly by its influence on the two neighboring As atoms at the surface. At large tip-sample distances, these As atoms show a reduced corrugation compared to the surrounding lattice, while at smaller tip-sample distances the corrugation is increased. This distance-dependent contrast inversion is explained by a relaxation of the As atoms above the defect which is induced by an attractive tip-sample interaction.

I. INTRODUCTION

InAs is a high-mobility, narrow-gap III-V semiconductor already used in many applications, e.g., infrared detectors[1] and Hall sensors.[2] Additionally, it is an essential part of several newly developed devices like mesoscopic heterostructures,[3] self-assembling quantum dots,[4] and hybrid ferromagnetic-semiconductor structures.[5] For the further development of such small devices and thin multilayer systems, where surface effects dominate over bulk properties, a detailed knowledge of the surface structure and their characteristics at the atomic scale is important. In particular, the investigation of point defects in semiconductors is an important matter, because they provide trap levels within the band gap, which determine many of their electric and optical properties.[6]

Up to now, real-space surface investigations on semiconductors on the atomic level have been carried out primarily with scanning tunneling microscopy (STM). Although this technique is very powerful, it suffers from two drawbacks. First, it is restricted to conducting samples, which becomes a serious problem for experiments at low temperature (i.e., experiments in high magnetic fields) on nondegenerate semiconductor surfaces. Second, STM in the constant current mode follows contour lines of the local density of states near the Fermi energy. Structural information is mixed with electronic information, especially in the vicinity of defects, where both the electronic structure close to the Fermi energy and the geometric structure of the atomic lattice change. Therefore, structural information cannot be extracted unambiguously from STM data.

Another method to investigate surfaces in real space is scanning force microscopy (SFM).[7] In 1995, Giessibl[8] showed that ''true'' atomic resolution[9] on Si(111)-(7×7) is possible with the dynamic mode of scanning force microscopy, which is also called noncontact atomic force microscopy. In this mode, the cantilever is oscillated at its resonant frequency f_{res} with a fixed amplitude A. Due to the tip-sample interaction, the oscillation frequency changes; the resulting frequency shift Δf is detected and used to drive the feedback electronics (constant frequency shift mode) as well as to record an image of the surface. In contrast to static contact SFM, a ''jump-to-contact'' can be prevented[10] and attractive short-range tip-sample interactions can be probed, which provide ''true'' atomic resolution, including the imaging of point defects. Note that long-range tip-sample interactions are also present, but do not contribute to contrast formation on the atomic scale. A significant advantage over STM is the ability to achieve ''true'' atomic resolution even on insulators.[11–13] Therefore, this method can be used on semiconductors in the whole range of doping concentrations and temperatures.

In this paper, we present an investigation of the (110) surface of n-InAs using the dynamic mode of SFM. After a short description of the experimental setup, we will first present our results on the defect-free surface and give an interpretation of the observed contrast, based on recent theoretical work. From this starting point, we will discuss the mechanisms that are responsible for contrast formation at and around two different types of atomically resolved point defects. The first point defect is located on the As sublattice and can be interpreted straightforwardly as an As vacancy. The second point defect, located on the In sublattice and showing a distance-dependent contrast inversion, is probably an In vacancy. To support our interpretations regarding the point defects, we will compare our results with experimental data and theoretical calculations on (110) surfaces of similar III-V semiconductors.[14]

II. EXPERIMENTAL SETUP

All measurements were carried out using our homebuilt scanning force microscope for ultrahigh-vacuum and low-

 ©2000 The American Physical Society

temperature applications, which is described in detail elsewhere.[15] The microscope was primerily designed to achieve atomic resolution in the static and dynamic mode likewise. Using low temperatures minimizes thermal drift and thereby ensures very stable imaging conditions. The peak-to-peak noise level is 10 pm in a 2-kHz bandwidth (see the line section of the raw data presented in Fig. 2), which corresponds to an rms noise below 2 pm. Such a high resolution is a prerequisite for precision measurements of structural properties at and around point defects, where height differences of only a few picometers are important. Furthermore, sensitive samples (InAs is prone to contamination) can be measured for several days without surface degradation.

The sample, an n-doped InAs single crystal (sulfur: $\approx 3\times 10^{18}$ cm^{-3}), was cleaved parallel to the (110) surface in the preparation chamber at pressures below 1×10^{-7} Pa, and immediately transferred into the precooled microscope located in the main chamber ($p<1\times 10^{-8}$ Pa). The whole microscope was then lowered into a bath cryostat and cooled until equilibrium temperature was reached. During most experiments both tip and sample were grounded. For measuremts with nonzero bias, the voltage was applied to the sample. The n-doped (antimony: 8×10^{17}–5×10^{18} cm^{-3}) silicon tips[16] used for the experiments were cleaned by argon sputtering. The cantilevers had spring constants of $k \approx 35$–38 N/m and showed eigenfrequencies of $f_0 \approx 160$–176 kHz. The instrument was operated in the dynamic mode, based on the frequency modulation technique,[17] keeping the frequency shift Δf as well as the oscillation amplitude A constant. The gray scale in all images throughout this paper is chosen in a way that bright areas represent stronger tip-sample interactions than dark areas (the tip-sample distance has to be increased in order to keep the frequency shift constant).

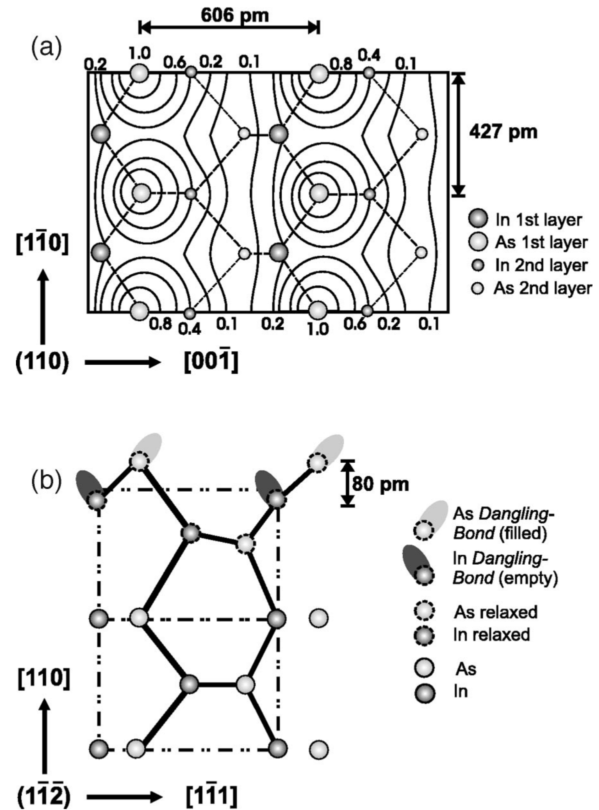

FIG. 1. (a) Top view on the (110) cleavage plane of InAs (bonds are indicated by dashed lines). The first-layer As and In atoms alternate in zigzag chains along the $[1\bar{1}0]$ direction. The lattice constants are $a=606$ pm in the [001] direction and $b=427$ pm in the $[1\bar{1}0]$ direction. The solid contour lines with the small numbers indicate a valence charge-density distribution approximately 0.3 nm above the surface. They are normalized with respect to the maximum value, which lies above the As. (b) Side view of the relaxed surface. The surface is As terminated, with the In atoms lying 80 pm below the As atoms. A charge transfer from the In dangling bonds to the As dangling bonds takes place. Both dangling bonds are tilted by $\approx 30°$, but in opposite directions (in the [001] and $[00\bar{1}]$ directions for the As and In dangling bonds, respectively).

III. CONTRAST FORMATION ON THE DEFECT-FREE SURFACE

InAs crystallizes in the ZnS structure, showing zigzag chains of alternating In (cations) and As (anions) atoms along the $[1\bar{1}0]$ direction [see Fig. 1(a)]. At the (110) surface, the As atoms relax outwards and the In atoms inwards, according to the bond rotation model, which is valid for most III-V semiconductors.[18] Therefore, the As sublattice is lifted by 80 pm above the In sublattice [see Fig. 1(b)]. The surface relaxation is accompanied by a charge transfer from the As dangling bonds to the In dangling bonds.

In most dynamic mode SFM images, rows of bright protrusions appear in atomic-scale images (see Fig. 2). Zigzag chains of alternating In and As atoms, as one might expect from the atomic structure displayed in Fig. 1(a), are usually not visible. The same observation was made by Sugawara *et al.* on InP(110).[19] The line section along the $[1\bar{1}0]$ direction in Fig. 2 demonstrates that the corrugation amplitude of 22 pm is easily resolved. The corrugation amplitude in the [001] direction is somewhat larger (26 pm), but largest in the $[1\bar{1}1]$ direction (48 pm).

Sometimes, however, two features per surface unit cell are imaged, as we already reported earlier.[20] Figure 3 shows two examples, which have been recorded with different cantilevers.[21] In both images, the second feature is visible between the bright protrusion: in (a), it manifests itself as a second, somewhat darker protrusion, while image b) exhibits a strongly localized depression at that position. The solid line sections elucidate their different characteristics along the [001] direction: In (a), the second feature has the shape of a shoulder ≈ 32 pm above the minima. In (b), an ≈ 5-pm-deep depression appears at the same position, which nearly reaches the level of the minima. The dashed line sections have also been taken along the [001] direction, but across the bright protrusions. Their profiles are very similar to each other, but the corrugation amplitudes are quite different: 75 pm in (a) and 18 pm in (b). The nearest perpendicular distance between the rows of bright protrusions and the rows of the second features is about 110 pm in both images, as indicated in the line sections. This value is in good agreement with the perpendicular distance between the rows of As and In atoms at the surface obtained from low-energy electron-diffraction experiments (100 pm)[22] and recent theoretical calculations (130 pm).[23]

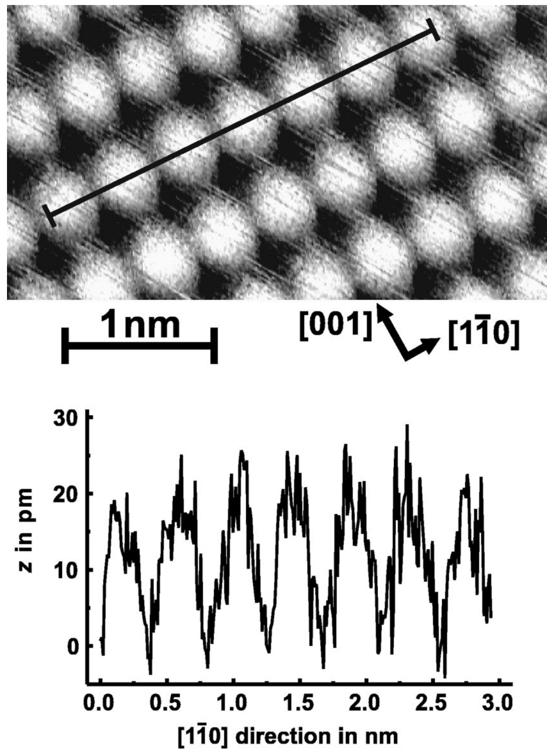

FIG. 2. Atomically resolved InAs(110)-(1×1) as typically imaged in dynamic scanning force microscopy (raw data). White protrusions represent the positions of the As atoms. The section along $[1\bar{1}0]$ shows a corrugation amplitude of ≈ 20 pm, and demonstrates that the peak-to-peak noise on the z piezo is about 10 pm ($\approx$2-pm rms) in a 2-kHz bandwidth. Parameters: $T=14$ K, $k\approx 36$ N/m, $f_{res}=160$ kHz, $A=\pm 12.7$ nm, $\Delta f=-55.3$ Hz, and $U_{bias}=+250$ mV.

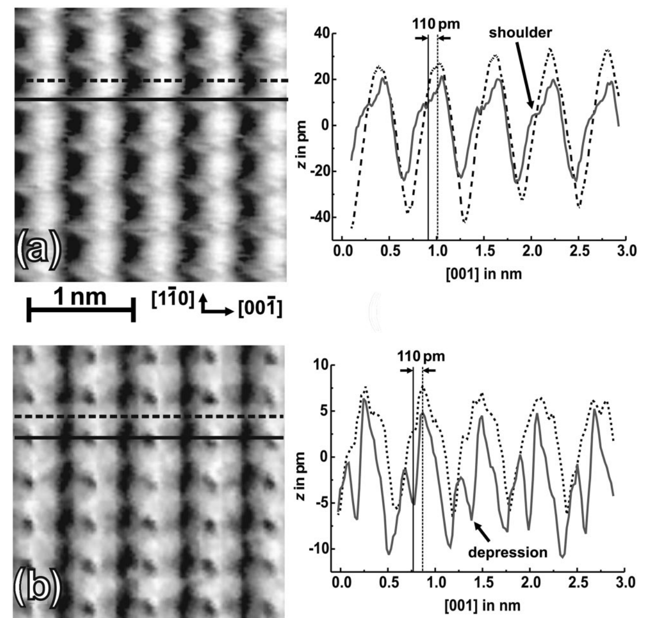

FIG. 3. Two examples of dynamic mode SFM images, where two features per surface unit cell are resolved on InAs(110)-(1×1). The bright protrusions are identified as the positions of the As atoms. The second feature, an additional protrusion in (a) and a depression in (b), is located between the bright protrusions, and can be attributed to the presence of the lower-lying In atoms. The line sections in the [001] direction across the bright protrusions (dashed line) and across the second feature (solid line) elucidate the different characteristic of the contrasts from the As and In atoms. A detailed explanation of the different characteristics is given in the text. Parameters: (a) $T=14$ K, $k\approx 36$ N/m, $f_{res}=160$ kHz, $A=\pm 12.7$ nm, and $\Delta f=-37.0$ Hz; (b) $T=78$ K, $k\approx 38$ N/m, $f_{res}=176$ kHz, $A=\pm 11.0$ nm, and $\Delta f=-447$ Hz.

How can these three different contrasts on InAs(110)-(1×1) be explained? An intuitive interpretation would lead to the conclusion that in Fig. 2 only one atomic species is imaged, while the two different maxima visible in Fig. 3(a) represent the zigzag configuration of the In and As atoms at the (110) surface. Since the surface is As terminated, one might identify the rows of bright protrusions in Figs. 2 and 3(a) as As atoms, while the somewhat darker protrusions are identified as the lower lying In atoms. The much higher corrugation amplitude in Fig. 3(a) compared to Fig. 2 indicates a smaller tip-sample distance, i.e., a stronger tip-sample interaction, which would support this interpretation. Moreover, even stronger support comes from *ex situ* x-ray-diffraction measurements on these samples, which show that if one accepts the bright protrusions to represent the positions of the As atoms, the In atoms have indeed to be located exactly at the positions of the somewhat darker maxima.

Care has to be taken with such a simple interpretation, which is based on purely structural arguments. As long as the quantity and the mechanisms, which govern the contrast formation, are unknown, it is *a priori* not clear how the features observed on atomic-scale images are related to the positions of the surface atoms.[24] This becomes immediately clear by comparing Figs. 3(a) and 3(b): Obviously, the second somewhat darker protrusion in (a) and the depression in (b) have the same relative position with respect to the bright maxima. This means that the same spot on the surface can exhibit completely different contrasts in dynamic mode SFM images. Therefore, a better understanding of the contrast mechanism is needed for a reliable interpretation of dynamic-mode SFM images.

To discuss this issue in more detail, we first determine the tip-sample distance relevant for contrast formation in atomic-scale images. For the measurement of a quantity that varies laterally on the atomic scale, the tip-sample distance has to be on the order of the interatomic distances, i.e., some one-tenth of a nanometer. Taking a typically chosen oscillation amplitude A of about ± 10 nm, the required tip-sample separation is only realized around the point of closest approach D. Güthner[25] was able to obtain atomic resolution with an oscillation amplitude of ± 10 nm on Si(111)-(7×7) in the dynamic mode of SFM and in the scanning tunneling mode simultaneously. Since a tunneling current only flows at a tip-sample distance of some tenths of a nanometer, this is a strong experimental indication that the point of closest approach D is indeed of this order.[26]

For such small tip-sample separations D and for $A \gg D$, Ke *et al.*[27] found that the frequency shift Δf is proportional to the geometric mean of the tip-sample potential $V_{int}(z)$ and the force $F_{ts}(z)=-\partial V_{int}(z)/\partial z$ between tip and sample at $z=D$, i.e., $\Delta f \propto \sqrt{|V_{int}(D) F_{ts}(D)|}$. With a different approach, U. D. Schwarz found the approximate analytical expression $\Delta f \propto V_{int}(z=D)/\sqrt{\lambda}$, with λ representing a characteristic decay length of $V_{int}(z)$ at $z=D$.[28] As long as the tip-sample

interaction force increases upon approach, both descriptions of the Δf dependence are approximately equivalent, because $\partial V_{\mathrm{int}}(z)/\partial z|_{z=D} \approx V_{\mathrm{int}}(D)/\lambda(D)$ for typical tip-sample potentials. It is important to note that for short-range interactions $\lambda \leqslant 0.1$ nm, i.e., the short-ranged contribution to the total tip-sample interaction will ideally only extend over the first atom at the tip apex.

In summary, contrast formation on the atomic scale in the dynamic mode of SFM is determined by the normal force between tip and sample and the tip-sample interaction potential at $D \approx 0.3-0.7$ nm.[29] Ciraci and co-workers[30,31] found that the total force between tip and sample $\vec{F}_{\mathrm{ts}}$ can be approximated by the sum of three different terms $\vec{F}_1$, $\vec{F}_2$, and $\vec{F}_3$, namely,

$$\vec{F}_1 = 2 \int \rho_s(\vec{r}) \sum_{t \in \mathrm{tip}} \frac{\partial}{\partial \vec{R}_t} \frac{Z_t}{|\vec{R}_t - \vec{r}|} d\vec{r}, \tag{1}$$

$$\vec{F}_2 = - \sum_{\substack{t \in \mathrm{tip} \\ s \in \mathrm{sample}}} \frac{\partial}{\partial \vec{R}_t} \frac{Z_t Z_s}{|\vec{R}_t - \vec{R}_s|} d\vec{r}, \tag{2}$$

and

$$\vec{F}_3 = 2 \int \Delta\rho(\vec{r}) \sum_{t \in \mathrm{tip}} \frac{\partial}{\partial \vec{R}_t} \frac{Z_t}{|\vec{R}_t - \vec{r}|} d\vec{r}, \tag{3}$$

where ρ_s denotes the valence charge density of the bare sample, $\Delta\rho$ the valence charge density modifacation due to the tip-sample interaction; $\vec{R}_t$ ($\vec{R}_s$) and $\vec{Z}_t$ ($\vec{R}_s$) are the position vector and the core charge of a tip (sample) ion.

Note that $\vec{F}_1$ is always attractive and $\vec{F}_2$ always repulsive, while the sign of $\vec{F}_3$ depends on the specific distribution of $\Delta\rho(\vec{r})$. For large tip-sample distances, $\vec{F}_1$ is almost compensated for by the ion-ion repulsion $\vec{F}_2$, while $\vec{F}_3$ vanishes, because $\Delta\rho$ becomes negligible. In this regime, the tip-sample interaction is dominated by long-range van der Waals forces. At small tip-sample distances, the strong ion-ion repulsion yields totally a repulsive force ($|\vec{F}_2| > |\vec{F}_1 + \vec{F}_3|$). In the intermediate regime, $|\vec{F}_1 + \vec{F}_3|$ decays more slowly than $|\vec{F}_2|$, leading to an electron-mediated attraction at $D \approx 0.3-0.7$ nm.[30,31]

Taking the three equations above, one can conclude that for $\rho_s \gg |\Delta\rho|$ and λ considerably smaller than the interatomic distances a_S at the surface, the positions of the maxima of the tip-sample interaction, and thus the positions of the maxima in dynamic mode SFM images, will be identical with the maxima of the valence charge density. Such a situation is, e.g., realized for metallic Al(001) ($a_S = 0.286$ nm $\gg \lambda$).[32] There, adhesive bond formation causes only small deviations from the total valence charge density of the undisturbed sample. Consequently, the interaction force has its maximum above the Al surface atoms, exactly where the total valence charge density has its maximum.[30]

On InAs(110), the interatomic distances between the surface As atoms are even larger than on Al(001). In Fig. 1(a), normalized contour lines of constant total valence charge density are plotted for InAs(110).[34] Above the As atoms, the total valence charge density has its maximum, while it is five times smaller at the position of the In atoms and has neither a (local) maximum nor a (local) minimum. Therefore, as long as $\rho_s \gg |\Delta\rho|$ is fullfilled, the protrusions in Fig. 2 can be straightforwardly interpreted as the positions of the As atoms, and the In atoms should remain invisible. This condition holds if either the tip-sample distance D is comparatively large (what might result in a low resolution) or if tip and sample do not form strong bonds, and seems to be realized more or less in most of the images [e.g., most of our data, including those presented here in the Figs. 2, 4, 5 and 6, and all images published for InP(110) in Ref. 19].

In contrast to the metallic Al(001) system mentioned above, the Si tip as well as the InAs(110) surface exhibit dangling bonds. Perez *et al.*[35] pointed out that these dangling bonds play an important role for contrast formation. For the case of a Si tip scanning over a Si(111)-(5×5) sample, they found that the attractive normal force and the tip-sample interaction energy is strongest above the adatoms, because the charge of tip and sample rearranges significantly (large $|\Delta\rho|$) and accumulates between the dangling bonds of the foremost Si tip atom and the dangling bond of the surface adatom, i.e., an ''onset of covalent binding'' occurs. Effects of this type led Ciraci and co-workers to the conclusion that even contrast reversal might occur for tip-sample systems, which form strong chemical bonds.[31] Therefore, it is important to reconsider the situation for configurations of the Si tip, which are able to form strong bonds with the InAs sample.

In the present case, the role of the dangling bonds has to be taken into account. Their orientation is depicted in Fig. 1(b): they are tilted by $\approx 30°$ in $[00\bar{1}]$ and [001] directions above the As atoms and In atoms, respectively. Consequently, the features on atomic-scale images might not be identical with the true atomic positions anymore, but might be slightly displaced in the [001] direction. However, such a displacement would be very small: even if the interaction would exclusively take place between the dangling bonds of the surface and the tip, the error would be below 10% of the length of the surface unit cell in the [001] direction (and zero in all other directions).[23] Therefore, the identification of atomic-scale features with the position of the surface atoms would still be a reasonably good approximation.

Let us now assume that the Si tip exhibits a reactive, but completely empty, dangling bond. If this dangling bond approaches the filled dangling bond of an As surface atom, the resulting strong interaction will lead to a comparatively large value of $|\Delta\rho|$: Charge will be displaced from the As atom toward the tip. As a consequence, $\vec{F}_3$ will be attractive, and the maximum at the position of the As atom will be even more enhanced.

At the position of the In atom, the interaction of the empty dangling bond of the Si tip and the empty dangling bond of the In atom will also lead to a net accumulation of charge between tip and sample, which, however, will probably not result in an attractive force of the same order as on top of the As atoms, since the charge which has to be displaced is not available within the bonds itself and has to be provided by the surrounding valence band. Nevertheless, the charge displacement will also cause an attractive force $\vec{F}_3$, and the position of the In atom might be visible as an additional, but

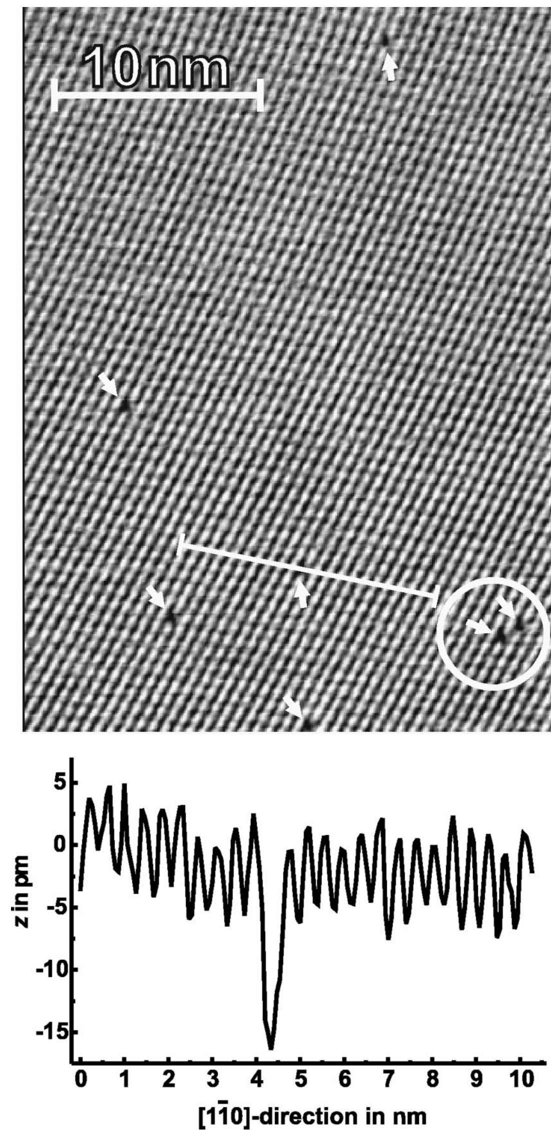

FIG. 4. Dynamic mode SFM image of InAs(110) with seven missing protrusions (white arrows) identified as As vacancies (see text). No lattice relaxation or an additional charge is visible around the vacancies. The line section shows a depression of about 15 pm instead of a protrusion at the position of the As vacancy. Parameters: $T = 14$ K, $k \approx 36$ N/m, $f_{\mathrm{res}} = 160$ kHz, $A = \pm 12.7$ nm, and $\Delta f = -63.2$ Hz.

smaller, protrusion. This scenario matches the experimental data presented in Fig. 3(a). The very high corrugation amplitude of 75 pm indicates the predicted enhancement of the corrugation amplitude above the positions of the As atoms. At the positions of the In atoms additional protrusions are visible, seen as a shoulders in the line section of Fig. 3(a).

On the other hand, a completely filled tip dangling bond also interacts strongly with the dangling bonds of the sample. If the tip dangling bond approaches the filled dangling bond of the As surface atom, charge has to be dislocated from the space between the Si tip atom and the As sample atom, leading to a negative $\Delta \rho$ in this area, and consequently to a repulsive force $\vec{F}_3$. Thus the maximum at the As atom position will diminish. At the position of the In atom, however, the filled tip dangling bond opposes the empty In dangling bond, and charge transfer from the tip toward the sample

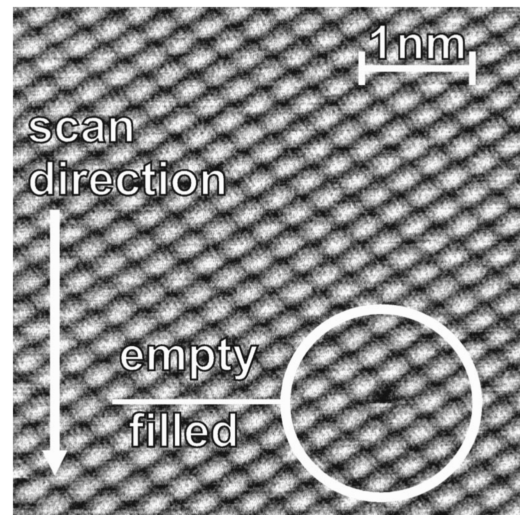

FIG. 5. High-resolution image of an As-site defect on InAs(110). During scanning from top to bottom, the As vacancy was moved; therefore, the As vacancy seems to be half-filled. The figure illustrates that the As atoms around an As vacancy do not relax within the resolution of our instrument. As in Fig. 4, no contrast induced by trapped charges is visible. Parameters: $T = 14$ K, $k \approx 36$ N/m, $f_{\mathrm{res}} = 156$ kHz, $A = \pm 13.5$ nm, and $\Delta f = -105.3$ Hz.

occurs. Since the charge can be moved comparatively easily, a repulsive force $\vec{F}_3$ of considerable strength is induced, and one would expect a well-expressed depression exactly at the position of the In dangling bond.

This second scenario corresponds nicely to the situation, as is found in Fig. 3(b). There, a depression localized precisely at the position of the In atoms is clearly visible [cf. the line section of Fig. 3(b)]. Additionally, the total corrugation height across the bright protrusions in the [001] direction is very low [only 18 pm compared to 48 pm in Fig. 2, and even 75 pm in Fig. 3(a)], which suggests that the predicted decrement of the height of the maximum at the As atom position really takes place. Therefore, to summarize the above findings, we have seen that the contrast mechanism in dynamic SFM is determined by electron-mediated attraction, which strongly depends both on the total valence charge density of the bare sample and on the ability of the tip to form bonds between tip and sample.

Finally, it is worth comparing the contrast mechanism of the dynamic mode of SFM described above with the contrast mechanism valid for STM on InAs(110) (or III-V semiconductors in general) at the atomic scale. Empty and filled states are localized at the cation sites and anion sites, respectively. Therefore, the contrast in STM strongly depends on the sign of the applied bias voltage on III-V semiconductors.[36] With a large positive sample bias the cation sublattice is imaged (tunneling from the STM tip into empty states), while the anion sublattice is imaged with large negative sample bias (tunneling from filled states into the STM tip). This general behavior on (110) surfaces of III-V semiconductors was also confirmed for InAs.[37] In our present case of dynamic-mode SFM, we checked that an electric field between the Si tip and the InAs sample, induced by the contact potential difference[38] or an applied bias voltage (± 1.8 V), did not influence the general appearance of the atomically resolved surface. However, any added (attrac-

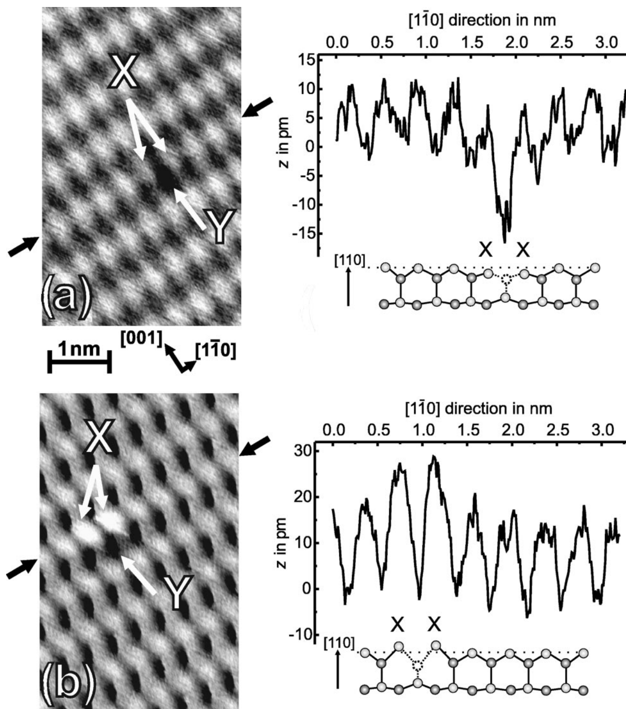

FIG. 6. Dynamic mode SFM image of a defect located on an In lattice site of InAs(110)-(1×1). In (a), the two As atoms marked with X (X sites) are displaced by 6 pm into the bulk (see the line section for illustration). In (b), the tip-sample distance is reduced by adjusting a larger negative frequency shift Δf, and the position of the defect is slightly shifted due to a different xy-offset voltage at the scan piezos. Now the X-site As atoms appear to be 10 pm higher than the surrounding As atoms (see the line section). This change is attributed to a stronger tip-sample interaction caused by the reduced tip-sample distance, which pulls the two weakly bound As atoms into the vacuum region. The sketches below the line sections indicate the tip-induced displacement of both X-site As atoms. Parameters: $T=14$ K, $k\approx 36$ N/m, $f_{\rm res}=160$ kHz, $A=\pm 12.7$ nm, (a) $\Delta f=-39.5$ Hz, and (b) $\Delta f=-44.7$ Hz.

tive) electrostatic contribution to the total tip-sample interaction had to be compensated for by an appropriate adjustment of Δf to assure a sufficiently small tip-sample distance to achieve atomic resolution.

This comparison shows that the origin of the tip-sample interaction is inherently different for STM and dynamic-mode SFM. Therefore, additional and/or complementary information is available with both methods. This will be further confirmed in the following sections, where the contrast at and around two different types of point defects will be discussed.

IV. POINT DEFECTS ON InAs(110)

A. As-site point defect

The most frequently observed type of point defect on freshly cleaved (110) surfaces was a missing protrusion. In Fig. 4, seven of such missing protrusions, marked by arrows, are visible. They are close to a cleavage step on the right-hand side of the image (not in the field of view). Far away from cleavage steps on n-InAs(110), we only occasionally found missing protrusions, but never with such a high density. The line section across one point defect shows that the protrusion is replaced by a 15-pm-deep depression. Since protrusions are associated with the positions of the As atoms, and these point defects are located on the As sublattice, they can be straightforwardly interpreted as As vacancies. The vacancies are probably formed during the cleavage procedure, which would explain their enhanced density close to the step edge.

At higher magnification, conclusions about the surface structure around the As vacancies can be drawn. The circled As lattice site in Fig. 5 is half-empty (upper part) and half-filled (lower part). The scan direction was from top to bottom. Apparently, this As lattice site had been a vacancy, which has probably been moved under the influence of the tip. In this context, it is interesting to compare the strength of the tip-sample interactions in Figs. 4 and 5. A measure for the tip-sample interaction is the normalized frequency shift $\gamma=\Delta f/f_0 kA^{3/2}$ introduced by Giessibl, which is independent of the parameter set (A,f_0,k) used during data acquisition.[10] Taking the parameters given in Fig. 5, γ can be estimated to $-38\ \mathrm{fNm}^{1/2}$, nearly twice as high as the γ calculated for the image displayed in Fig. 4 ($-20\ \mathrm{fNm}^{1/2}$). This might be the reason why the vacancy in Fig. 5 is moved by the tip, but those in Fig. 4 are not. Other possible explanations are less plausible: Thermal activation is unlikely at 14 K, and desorption of an As atom from the tip or a tip change would not give such a smooth transition from an empty to a filled As lattice site as in the image.

Comparing the upper half of the circle in Fig. 5 (the empty As lattice site) with the lower half (filled As lattice site), it can be concluded that the As atoms around an As vacancy do not relax significantly. All distances between protrusions and the corrugation amplitudes of the protrusions remain the same within the resolution of our instrument. Note that we do not image the In sublattice here; therefore, a relaxation of the surrounding In atoms cannot be excluded. This finding is in agreement with results from G. Schwarz *et al.*, who calculated for GaP(110) that the relaxation around a surface anion vacancy (P vacancy) is restricted to the nearest-neighbor cations.[39]

Furthermore, it can be concluded from both Figs. 4 and 5 that the As vacancies are not charged. With STM, charge clouds were found around charged vacancies on various III-V semiconductors.[37,40,41] The screened Coulomb potential of a charged vacancy should lead to an additional electrostatic contribution to the total tip-sample interaction in a circular area with a radius in the order of the screening length ($\lambda_S\approx 8$ nm in our case) around the vacancy, which we never observed around As vacancies on n-InAs(110). Moreover, Ebert et al.[42] observed on InP(110) and GaP(110) that charged vacancies induce displacements up to two lattice constants away from the defect, while neutral anion vacancies do not induce such a relaxation in the anion sublattice in their vicinity. They also exhibited no charge cloud around them. Neither a charge cloud, nor any distortions of the As sublattice, are visible around the vacancies in our measurements. An additional argument is that charged As vacancies would repel each other.[43] However, the two vacancies encircled in Fig. 4 are very close together.

It is worth noting that in spite of the fact that images of neutral anion vacancies acquired on similar III-V semiconductors with STM and dynamic mode SFM on InAs(110)

look quite similar, the origin of the contrast is different. In STM, the missing filled dangling bond of an anion vacancy leads to a reduced tunneling current at negative sample bias, which manifests itself in a depression. However, the contrast changes with the sign and magnitude of the applied bias voltage.[42] In dynamic-mode SFM, an As vacancy also results in a depression, because the missing As atom leads to a reduced charge density at that spot and leaves a geometrical hole behind. Thus, compared to STM measurements, dynamic-mode SFM gives a more direct and intuitive view of the surface geometry at and around anion vacancies.

B. In-site point defect

In Fig. 6, a different type of point defect is presented. Both parts (a) and (b) of the figure show the same point defect on the sample recorded with a different frequency shift Δf. The lower-frequency shift in Fig. 6(b) corresponds to a decreased tip-sample distance and consequently to a stronger (attractive) tip-sample interaction than in Fig. 6(a). Accordingly, the corrugation amplitude in the $[1\bar{1}0]$ direction of the unperturbed lattice increases from 10 pm in (a) to 20 pm in (b). The increased tip-sample interaction causes a contrast inversion at the defect, namely, at the neighboring atoms marked with *X*. In (a), the maxima of the *X*-site protrusions appear ≈ 6 pm below the surrounding As sublattice, while in (b) they appear ≈ 10 pm above the surrounding As atoms. Moreover, the depression at *Y* is deeper [by 9 pm (a) and 6 pm (b), respectively] compared to the equivalent undisturbed lattice sites.

It is not possible to specify the type of point defect exactly, but most commonly occurring point defects can be ruled out. Adsorbates appeared much more broadened and never so localized. Two neighboring impurities on As lattice sites are very unlikely, and would induce a larger lattice distortion. Therefore, we assume that the *X* sites are actually two As atoms influenced by a defect between them. Because of the mirror symmetry with respect to the [001] direction, this point defect must be located on the In lattice below both *X* sites. The different symmetry with respect to the As surface atoms of interstitial atoms and subsurface defects located on As sites would probably lead to a different appearance of the two As atoms at the *X* sites. Such a defect on the In site could be an impurity atom, an antisite defect, or an In vacancy. The latter is supported by the deep depression at *Y* (see below).

How can this contrast inversion occur? The simulation of the scanning process by Perez *et al.* revealed that surface atoms can be significantly displaced during scanning.[35] Chou and Joannopoulos calculated that a SFM tip is able to flip the orientation of Si dimers on Si(100), and that this should be observable at low temperatures.[44] A defect below the As atoms on the *X* sites, especially a missing In atom, would weaken the stiffness of the surrounding lattice. Considering this, an additional attractive tip-sample interaction might provide enough energy to pull the two weakly bonded As atoms above the In site defect toward the tip, e.g., into the vacuum region. These local changes in the lattice parameters reflect the different elastic properties around the point defect compared to the undisturbed lattice.

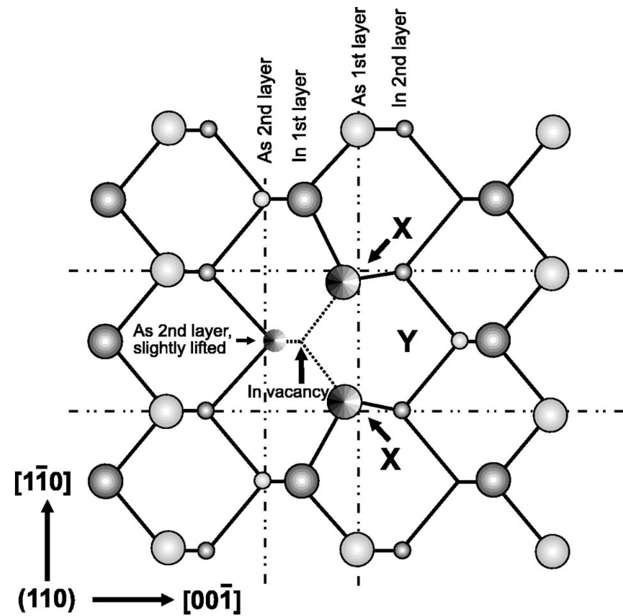

FIG. 7. Top view of the proposed relaxation around an In vacancy, as derived in analogy to GaP(110) from Ref. 39. All three neighboring As atoms are displaced in such a manner that the distances between them are reduced. For a cation vacancy in GaP(110), the total displacement of the first (second) layer anions is 82 pm (56 pm) (see Ref. 39). Due to the relaxation, the tip can penetrate deeper at *Y* than at the location of the In vacancy.

This scenario is consistent with calculations from G. Schwarz *et al.* for cation vacancies (Ga vacancies) on GaP(110).[39] They found that the two anions above the cation vacancy would relax downwards, exactly like in Fig. 6(a) for a relatively weak attractive tip-sample interaction. However, their calculated downward relaxation of 44 pm is much deeper than the 6 pm measured in Fig. 6(a). Three explanations could account for this. First, the downward relaxation for a cation vacancy could be much smaller for InAs(110) than for GaP(110) (they are similar, but not equal, materials). Second, the defect might not be a vacancy, but an impurity or an antisite defect, resulting in a much smaller downward relaxation (no calculations for this case exist). Third, the attractive tip-sample interaction necessary for a substantial tip-induced relaxation could already be present at larger tip-sample distances (this might happen in addition to the first or second argument).

From Sec. III, we know that the In lattice site is not located at *Y*, but on the other side of the two *X*-site As atoms. However, surprisingly the depression is deepest at *Y*, while at the real position of the In-site defect, the depression is only 2 pm deeper in (a) and has the same level as the undisturbed lattice in (b). This could be explained with a simple geometrical reasoning, which favors the assumption that the observed point defect represents an In vacancy. In this case, as visualized in Fig. 7, all three neighboring As atoms move closer together. Such a relaxation has been found in the calculation for the Ga (cation) vacancy on GaP(110) already mentioned above.[39] The effect is a reduction of the interatomic distances between the As atoms of the first- and second-layer As atoms around the In vacancy. Consequently, on the other side of the two relaxed first-layer (*X*-site) As atoms (at the *Y* site) the charge density is reduced, i.e., more

''space'' becomes available, and the tip can penetrate deeper into the surface. As in the case of the As vacancy, this defect appears to be neutral at zero bias (same arguments as given in Sec. IV A for the charge state of the As vacancy). A sample bias of +250 mV did not change the contrast, but, as already stated in Sec. III, Δf had to be readjusted to achieve atomic resolution.

It is again instructive to compare our data with results obtained by STM. As in the case of anion vacancies, experiments on neutral cation vacancies on GaP(110) exhibited a strong dependence on sign and magnitude of the applied bias voltage.[45] At negative bias voltages all four surrounding anions at the surface are influenced by the presence of a cation vacancy. However, our data, and theoretical calculations by Schwarz *et al.*[39] suggest that only two anions are significantly relaxed downwards. Nevertheless, the dynamic-mode SFM results presented in this section demonstrate that also with this method quantitative structural information around defects cannot be extracted unambiguously, since tip-induced relaxations have to be considered even in the attractive interaction regime. On the other hand, the observed tip-induced relaxation shows that elastic data on the atomic level can be obtained from dynamic-mode SFM data.

V. SUMMARY

We presented results of an atomic-scale study of the InAs(110)-(1×1) surface by means of dynamic-mode SFM performed at low temperatures and in UHV. It was shown that dynamic scanning force microscopy images the surface As atoms as bright protrusions. However, under certain circumstances both species are visible. The observed contrast can be qualitatively explained with the total valence charge density at the surface and the rearrangement of the charge distribution due to the tip-sample interaction.

Missing protrusions in the As sublattice are straightforwardly identified as As vacancies. It was found that As vacancies do not induce a measurable relaxation in the surrounding As sublattice. Furthermore, they appeared neutral on *n*-doped material under our experimental conditions (zero bias).

Another point defect, located on the In sublattice, could be detected by its influence on two neighboring surface As atoms. These As atoms exhibited a distance-dependent contrast inversion, attributed to a tip-induced relaxation. Symmetry arguments suggest that the defect is located on the In sublattice. The contrast around the defect could be best explained by an In vacancy. The observed relaxation gives evidence that elastic properties can be measured on the atomic scale with dynamic-mode SFM.

ACKNOWLEDGMENTS

The authors would like to thank Phillip Ebert, Markus Morgenstern, Hendrik Hölscher, and Günther Schwarz for helpful discussions, and Livio Fornasio for the determination of the crystal orientation by x-ray-diffraction measurements. Financial support from the VW foundation (Grant No. I/69 649), the BMBF (Grant No. 13N6921/3), and the Graduiertenkolleg ''Physik nanostrukturierter Festkörper'' is gratefully acknowledged.

[1] M. E. Greiner and C. J. Martin, Proc. SPIE **686**, 34 (1989).

[2] N. Kuze and I. Shibasaki, III-V's Rev. **10**, 28 (1997).

[3] J. M. Klapwijk, Physica B **197**, 481 (1994).

[4] P. M. Petroff and S. P. DenBaars, Superlattices Microstruct. **15**, 15 (1994).

[5] M. Johnson, B. R. Bennett, M. J. Yang, M. M. Miller, and B. V. Shanabrook, Appl. Phys. Lett. **71**, 974 (1997).

[6] H. J. Queisser and E. E. Haller, Science **281**, 945 (1998).

[7] G. Binnig, C. F. Quate, and C. Gerber, Phys. Rev. Lett. **56**, 930 (1986).

[8] F. J. Giessibl, Science **267**, 68 (1995).

[9] In the contact mode of SFM, only the translational symmetry of the surface is reproduced on an atomic scale. The contrast formation is governed by frictional forces, and point defects cannot be detected for fundamental reasons.

[10] F. J. Giessibl, Phys. Rev. B **56**, 16 010 (1997).

[11] M. Bammerlin, R. Lüthi, E. Meyer, A. Baratoff, J. Lü, M. Guggisberg, C. Gerber, L. Howald, and H.-J. Güntherodt, Probe Microsc. **1**, 3 (1997).

[12] K. Fukui, H. Onishi, Y. Iwasawa, Phys. Rev. Lett. **79**, 4202 (1997).

[13] W. Allers, A. Schwarz, U. D. Schwarz, and R. Wiesendanger, Europhys. Lett. **48**, 276 (1999).

[14] This is justified since the surface structures of all these materials are very similar. That is, all materials relax qualitatively in the same way; only the absolute values of the displacements are slightly different.

[15] W. Allers, A. Schwarz, U. D. Schwarz, and R. Wiesendanger, Rev. Sci. Instrum. **69**, 221 (1998).

[16] Nanosensors, Aidlingen, Germany.

[17] T. R. Albrecht, P. Grütter, D. Horne, and D. Rugar, J. Appl. Phys. **42-44**, 668 (1992).

[18] That is, all phosphides [e.g., GaP(110) and InP(110)], arsenides [e.g., GaAs(110)], as well as most antimonides.

[19] Y. Sugawara, M. Ohta, H. Ueyama, and S. Morita, Science **270**, 1646 (1995).

[20] A. Schwarz, W. Allers, U. D. Schwarz, and R. Wiesendanger, Appl. Surf. Sci. **140**, 293 (1999).

[21] Note that the adjusted frequency shift Δf is much larger for (b) than for (a). However, this is not extraordinary for different cantilvers, and it is not possible to deduce that the tip-sample interaction relevant for atomic resolution is stronger in one image or the other.

[22] C. B. Duke, C. Mailhot, A. Paton, D. J. Chadi, A. Khan, J. Vac. Sci. Technol. B **3**, 1087 (1985).

[23] B. Engels, Ph. D. thesis, RWTH Aachen, KFA Jülich, 1996.

[24] In the static contact mode of SFM, this issue has been an open question for a long time. Finally, it has been accepted that atomic-scale images are dominated by frictional forces, and that protrusions in the images are not necessarily identical with atomic positions.

[25] P. Güthner, J. Vac. Sci. Technol. B **24**, 2428 (1996).

[26] For simultaneous recording of a dynamic mode SFM image and a

STM image, the bandwidth of the current preamplifier has to be much smaller than the frequency of the cantilever oscillation (30 and 290 kHz, respectively, in Ref. 25).

[27] S. H. Ke, T. Uda, and K. Terakura, Phys. Rev. B **59**, 13 267 (1999).

[28] U. D. Schwarz, Habilitation thesis, University of Hamburg, 1999.

[29] In previous publications, it was often stated that the force derivative is the quantity which influences the frequency of the cantilever (e.g., Refs. 8, 19, and 35). This is only valid for tip-sample interactions which do not vary significantly over the whole oscillation cycle, and therfore represents a reasonable approximation only for long-range forces. For atomic-scale imaging, where short-range forces are probed, such an assumption is not valid [see H. Hölscher, U. D. Schwarz, and R. Wiesendanger, Appl. Surf. Sci. **140**, 344 (1999)].

[30] S. Ciraci, E. Tekman, A. Baratoff, and I. P. Batra, Phys. Rev. B **42**, 10 411 (1992).

[31] S. Ciraci, in *Forces in Scanning Probe Methods*, edited by H.-J. Güntherodt, D. Anselmetti, and E. Meyer (Kluwer, Dordrecht, 1995), pp. 133–147.

[32] At this point, it is important to note that the maximum of the valence charge density is not in every case identical with the largest attractive interaction force, even if $\rho_{s} \gg |\Delta\rho|$. If the interatomic distances a_S are very small, i.e. about comparable to the characteristic decay length λ of the interaction, the influence of neighbor atoms on the tip has to be considered. This situation is, e.g., realized within the surface structure of graphite(0001) (see Ref. 33). The in-plane nearest-neighbor distance between the graphite atoms is very small ($a_S = 142$ pm), and integration leads to a largest attractive force $\vec{F}_{ts}$ above the hollow sites of the honeycomb structure, where all six surrounding graphite atoms contribute to the tip-sample interaction. However, such an effect can be excluded for InAs(110), since the interatomic distances between the surface As atoms are much larger.

[33] S. Ciraci, E. Tekman, and I. P. Batra, Phys. Rev. B **41**, 2763 (1990).

[34] The total valence charge density has been taken from Ref. 23. The distribution is very similar for all (110) surface of III-V semiconductors with ZnS structure, and decays exponentially at larger tip-sample distances.

[35] R. Perez, M. C. Payne, I. Stich, and K. Terakura, Phys. Rev. Lett. **78**, 678 (1997); R. Perez, I. Stich, M. C. Payne, and K. Terakura, Phys. Rev. B **58**, 10 835 (1998).

[36] R. M. Feenstra, J. A. Stroscio, J. Tersoff, and A. P. Fein, Phys. Rev. Lett. **58**, 1192 (1987).

[37] A. Depuydt, N. S. Maslova, V. I. Panov, V. V. Rakov, S. V. Savinov, and C. Van Haesendonck, Appl. Phys. A **66**, 171 (1998).

[38] The work functions of *n*-InAs(110) and Si are both ≈ 4.90 eV, resulting in a contact potential difference close to zero. Nevertheless, due to the tip geometry, the work function of the Si tip will be reduced. The problem of determining precisely the contact potential difference between *n*-InAs(110) and a Si tip is neither trivial nor of major interest for the present purpose, and will be discussed in a forthcoming paper.

[39] G. Schwarz, A. Kley, J. Neugebauer, and M. Scheffler, Phys. Rev. B **58**, 1392 (1998).

[40] P. Ebert and K. Urban, Ultramicroscopy **49**, 344 (1993).

[41] P. Ebert, M. Heinrich, M. Simon, C. Domke, K. Urban, C. K. Shih, M. B. Webb, and M. G. Lagally, Phys. Rev. B **72**, 4580 (1996).

[42] P. Ebert, K. Urban, and M. G. Lagally, Phys. Rev. Lett. **72**, 840 (1994).

[43] Note that the measurement in Figs. 4 and 5 were done with zero bias, and that the actual charge state of a vacancy generally depends on the sign and absolute value of an applied bias voltage.

[44] K. Chou and J. D. Joannopoulos, Surf. Sci. **328**, 320 (1995).

[45] P. Ebert and K. Urban, Phys. Rev. B **58**, 1401 (1998).